



ACADEMIC  
PRESS

Biochemical and Biophysical Research Communications 295 (2002) 636–643

BBRC

www.academicpress.com

## Membrane fusion induced by the major lipid-binding domain of the cytoskeletal protein talin<sup>☆</sup>

Gerhard Isenberg,<sup>a</sup> Sabine Doerhoefer,<sup>a</sup> Dick Hoekstra,<sup>b</sup> and Wolfgang H. Goldmann<sup>c,\*</sup>

<sup>a</sup> Department of Biophysics E22, Technical University Munich, James-Franck-Str., D-85748 Garching, Germany

<sup>b</sup> Department of Physiological Chemistry, University of Groningen, Antonius Deusinglaan 1, 9713 AV Groningen, Netherlands

<sup>c</sup> Department of Medicine, Renal Unit, Massachusetts General Hospital, Harvard Medical School, Bldg. 149, 13th St., Rm. 8200, Charlestown, MA 02129, USA

Received 10 June 2002

### Abstract

Secondary structure predictions have led to the identification of a major membrane-anchoring domain of the cytoskeletal protein talin spanning from amino acid 385 to 406. Using a synthetically derived peptide of this region, researchers have shown that it inserts into POPC/POPG phospholipid membranes with a partition coefficient of  $K_{app} = 1.1 \pm 0.2 \times 10^5 M^{-1}$  and has an average molar reaction enthalpy of  $\Delta H = -2.5$  kcal/mol, as determined by monolayer expansion technique and isothermic titration calorimetry [J. Biol. Chem. 275, 17954]. We applied resonance energy transfer (RET) assays to analyze the fusogenic properties of this peptide by lipid mixing and used liposomes containing carboxyfluorescein to measure the contents leakage. We directly visualized talin peptide-induced vesicle membrane fusion using cryo-electron microscopy. This is the first example of a cytoskeletal protein domain that can trigger membrane fusion that might be of importance for understanding membrane targeting and motile events at the leading edge of the cell. © 2002 Elsevier Science (USA). All rights reserved.

Talin is a member of the 4.1 superfamily, a group of proteins that potentially associates with phospholipid membranes. To this group also belong the erythrocyte membrane protein 4.1 [1], the ezrin, radixin, moesin family [2], and some tyrosine phosphatases [3]. Talin is a widespread protein that is found in a variety of mammalian cells, where it is concentrated in focal cell adhesions [4] and ruffling membranes [5]. In platelets, talin redistributes from the cytoplasm to the plasma membrane upon activation, leading to secretory events and platelet coagulation via integrins [6], a complex process that is not fully understood. Several divergent binding epitopes have been mapped along the entire sequence of

2541 amino acids [1], suggesting that talin may be a multifunctional protein. Calpain cleavage before amino acid residue 434 yields two major domains, an N-terminal head portion of 47-kDa and a 190-kDa rod domain containing the C-terminus. Talin is also found to bind actin [7,8] and to nucleate actin polymerization [9]. From in vitro studies, the functional actin-binding capacity was shown to be restricted to the C-terminal rod domain [10]. Consequently, GST-fusion proteins were used to map two actin-binding regions in the 190-kDa talin fragment [11], termed the I/LWEQ module based on their conserved sequences [12]. An additional actin-binding site was found in the 47-kDa head fragment [11], which may be cryptic or inaccessible since no actin-binding was observed within this part of the native protein [10,13]. In addition to actin, the C-terminal rod domain harbors binding sites for integrin [14,15] and vinculin [16]. The 47-kDa head fragment is believed to be of major importance for talin's association with the plasma membrane. Recently, binding sites for two independent transmembrane proteins, laylin [17], and integrin  $\beta$ -subunit cytoplasmic domain [18] have been identified in this fragment. Phospholipid binding has

<sup>☆</sup> Abbreviations: DPPE, 1- $\alpha$ -dipalmitoylphosphatidylethanolamine; DPA, pyridine-2,6-dicarboxylic acid; PE-PDP, *N*-succinimidyl 3-(2-pyridylthio)propionate-derivatized DPPE; N-NBD-PE, *N*-(7-nitro-2,1,3-benzoxadiazol-4-yl)phosphatidylethanolamine; N-Rh-PE, *N*-(lissamine rhodamine B sulfonyl)dihexadecanoyl-sn-glycero-3-phosphatidylethanolamine; DOPS, dioleoylphosphatidylserine; DOPC, dioleoylphosphatidylcholine; RET, resonance energy transfer; CF, 6-carboxyfluorescein.

\* Corresponding author. Fax: +1-617-726-5671.

E-mail address: wgoldmann@partners.org (W.H. Goldmann).

also been shown to be exclusively mediated by the 47-kDa domain [10].

Our laboratory successfully applied the secondary structure prediction method based on the Eisenberg normalized consensus scale to search for highly hydrophobic or amphipathic sequence stretches that could mediate the binding of actin-associated proteins with phospholipid membranes [19]. For talin, two domains spanning amino acid residues 21–39 and 385–406 were identified that mediate the interaction with lipid membranes [20]. These peptides were synthesized and their insertion into lipid model membranes was probed using isothermic titration calorimetry (ITC), the monolayer expansion technique, and CD-spectroscopy. In the presence of lipids, the major membrane-binding peptide, i.e., residue 385–406 refolds from a random coil into an  $\alpha$ -helix. Simultaneous insertion into a bilayer leaflet occurs with a measured hydrophobic partition coefficients of  $K_p = 1.3 \pm 0.2 \times 10^4 \text{ M}^{-1}$ , a value that agrees well with partition coefficients determined for myristoylated proteins such as hisactophilin and  $\alpha$ -transducin.

In this study, we further analyze the membrane-anchoring peptide of talin. Peptides with a high degree of hydrophobicity, a high degree of amphipathicity, and tilted insertion are classified peptides as ‘class B peptides.’ These peptides preferentially destabilize phospholipid bilayers and lead to inverted micelle formation favoring membrane fusion. Applying various assay systems that allow us to control for lipid-mixing events or contents leakage, we found evidence that the talin peptide indeed is fusogenic. Finally, we demonstrated talin peptide-induced fusion of lipid vesicle membranes using cryo-electron microscopy.

## Materials and methods

**Chemicals.** 1- $\alpha$ -Dipalmitoylphosphatidylethanolamine (DPPE), *N*-succinimidyl 3-(2-pyridyl)dithio)propionate (SPDP), cholesterol (chol), dipicolinic acid (pyridine-2,6-dicarboxylic acid, DPA), and Triton X-100 were obtained from Sigma. SPDP-derivatized DPPE (PE-PDP) was synthesized as described earlier [21].  $\text{TbCl}_3 \cdot 6\text{H}_2\text{O}$  (99.9% pure) was bought from Alfa. The fluorescent lipid analogs *N*-(7-nitro-2,1,3-benzoxadiazol-4-yl)phosphatidylethanolamine (N-NBD-PE) and *N*-(lissamine rhodamine B sulfonyl)dihexadecanoyl-sn-glycero-3-phosphatidylethanolamine (N-Rh-PE) as well as 6-carboxyfluorescein were purchased from Molecular Probes. Sodium dithionite was purchased from Merck. Dioleoylphosphatidylserine (DOPS) and dioleoylphosphatidylcholine (DOPC) were obtained from Avanti Polar Lipids. The detergent  $\text{C}_{12}\text{E}_8$  was supplied by Calbiochem.

**Peptide synthesis.** Talin peptide 385–406 GEQIAQLIAGYI DIILK K K K KSK-CONH<sub>2</sub> (MW 2457,02) was synthesized by continuous flow Fmoc solid phase (Bio Genes, Berlin) as trifluoroacetate salts. The peptide was purified by reversed phase HPLC and analyzed by mass spectroscopy. To induce irreversible coupling with phospholipids, we added an additional cysteine (Cys) to the sequence on the C-terminal end (data not shown). The grade of purity was  $\geq 95\%$  for each sample. Peptide stock solutions were stored at  $-20^\circ\text{C}$  or used immediately.

**Liposome preparation.** All liposomes were prepared by the method described by Pêcheur et al. [22]. Their average diameter was 100–150 nm. Peptide-coupled liposomes, which were defined as donor liposomes throughout the study, consisted of PC:chol:PE-PDP (3.5:1.5:0.25). Coupling was accomplished via disulfide bonding between the peptide’s Cys residue and PE-PDP. It was obtained by an overnight conjugation of the peptide talin with the liposomes (PE-PDP/peptide in a 1:5 molar ratio). The coupling efficiency was evaluated spectrophotometrically at 343 nm by monitoring the release of 2-mercaptopyridine. Uncoupled peptides were removed by gel filtration on a Sephadex G-25 column (PD-10 column, Amersham/Pharmacia). Target liposomes were composed of DOPC, DOPS, or DOPC/DOPS (at a molar ratio of 1:1).

**Resonance energy transfer (RET) assay for lipid mixing.** Lipid mixing of vesicles—as a measure of fusion—was assayed as described by Struck et al. [23]. Target vesicles were added to a suspension of peptide-coupled liposomes containing N-NBD-PE and N-Rh-PE (1 mol% each) in 10 mM Tris and 150 mM NaCl (pH 7.4) at a lipid molar ratio of 5:1 (total lipid concentration of 70  $\mu\text{M}$ ). The increase in NBD fluorescence was monitored at 37  $^\circ\text{C}$  as a function of time in a Fluorolog fluorimeter (SPEX) ( $\lambda_{\text{exc}} = 460 \text{ nm}$ ,  $\lambda_{\text{em}} = 534 \text{ nm}$ ) at continuous stirring. The temperature was controlled by a thermostated circulating water bath. Zero percent and 100% fluorescence were taken as the intrinsic fluorescence intensity of NBD/Rh-labeled liposomes and the fluorescence obtained after addition of 0.2% Triton X-100 (final concentration) was corrected for detergent-induced quenching of NBD fluorescence, respectively.

Asymmetrically labeled vesicles, i.e., containing N-NBD-PE in the inner leaflet only, were prepared by incubating randomly labeled vesicles with 20 mM sodium dithionite for 20 min at 37  $^\circ\text{C}$  [24]. This treatment irreversibly destroys the NBD fluorescence via a reduction reaction [25] and eliminates the fluorescence signal derived from N-NBD-PE present in the outer leaflet, thus leading to an intensity decrease of approximately 50–60%. Sodium dithionite-treated liposomes were separated from un-reacted dithionite by elution on a Sephadex G-25 column (PD-10 column, Amersham/Pharmacia). Subsequent addition of Triton X-100 allowed additional access of thionite to the inner leaflet, which is reflected by an immediate quenching of the remaining fluorescence.

**Leakage assays.** Talin peptide-induced leakage was determined by adding peptide-coupled liposomes to a suspension of target vesicles loaded with 100 mM carboxyfluorescein (CF) in 10 mM Tris and 150 mM NaCl at pH 7.4. Fluorescent marker release was measured by a method analogous to that of Weinstein et al. [26] (excitation 490 nm; emission 520 nm). The internal concentration of the dye was high enough to quench the fluorescence almost completely. Release of CF led to an increase of fluorescence intensity, which was compared with the value obtained after addition of Triton X-100 (final concentration about 0.4%).

**Cryo-electron microscopy.** In lipid-mixing assays, DOPC/DOPS target liposomes (molar ratio of 1:1) were added to DOPC/cholesterol donor liposomes without the fluorescent phospholipids (molar ratio of 3.5:1.5) at a total lipid molar ratio of 5:1 in the presence of 20  $\mu\text{M}$  synthetic talin peptide. After 45 and 160 s, respectively, 5  $\mu\text{l}$  aliquots were applied to Lacey holey carbon EM-grids (Plano, Wetzlar, Germany). Excessive liquid was blotted on filter paper to a thickness less than 200 nm and the specimens were plunged into liquid ethane at  $-190^\circ\text{C}$  [27]. The grids were transferred to a Gatan 626 cryo-specimen holder (Gatan, Pleasanton, CA) and inserted into a Philips CM 300 FEG (FEI Company, Hillsboro, OR) electron microscope under liquid nitrogen conditions. The post-column energy filter GIF 2002 (Gatan, Pleasanton, CA) attached to the microscope enhances the contrast of the images as inelastically scattered electrons are masked from the zero-loss electron beam [28]. The electrons are detected on a 2048  $\times$  2048 CCD chip. The images are recorded at magnifications of 14,000 $\times$  or 22,000 $\times$  corresponding to pixel sizes of 0.85 and 0.58 nm, respectively.

**Hydrophobicity calculations and molecular modeling.** The mean hydrophobicity and mean hydrophobic moments were calculated according to the Eisenberg consensus scale [29] allowing for the prediction of a three-dimensional mode of insertion and orientation of the amphipathic  $\alpha$ -helical anchoring peptide. Computations were performed using the PC-TAMMO+ program (Theoretical Analysis of Molecular Membrane Organization) as described by Brasseur [30], which takes into account the sum of the van der Waal's forces, torsion potential energy, electrostatic interactions, and the transfer energy between peptide and DMPG in the lipid layer. The angle of insertion was calculated according to Brasseur et al. [31].

## Results

To determine whether the intrinsic membrane-anchoring domain of talin (amino acid 385–406) could trigger membrane fusion, various assays were applied based on lipid-mixing and contents leakage. Consistent with the previous notion that talin as a whole [32,33] as well as the peptide alone [20] preferentially inserts into lipid mono- and bilayers containing negatively charged phospholipids, we used target liposomes composed of a total lipid concentration of 70  $\mu$ M DOPS or DOPC/DOPS at a molar ratio of 1:1. The fusogenic potential of

the peptide was examined under a variety of conditions: (a) the talin peptide was applied free in solution; (b) the cysteine-derivatized peptide was applied in solution; and (c) the peptide was covalently coupled with donor-liposomes containing PE-PDP via an additional cysteine (see Materials and methods).

### Fusion monitored by lipid mixing

DOPC/cholesterol donor liposomes were prepared containing NBD- and rhodamine-labeled phospholipids. Internal quenching of the liposome surface resulted in a low baseline fluorescence. Donor liposomes were mixed with DOPC/DOPS target liposomes at a ratio of 1:5 in the presence of increasing concentrations of the talin peptide in solution (Fig. 1).

Membrane fusion results in lipid mixing, which causes dequenching and hence a rapid increase in fluorescence with increasing surface area. An increase of fluorescence is observed after adding the talin peptide in a concentration-dependent manner (Fig. 1A). Fig. 1B shows the effect on lipid mixing after the addition of liposomal-coupled peptide using DOPS or DOPC/DOPS

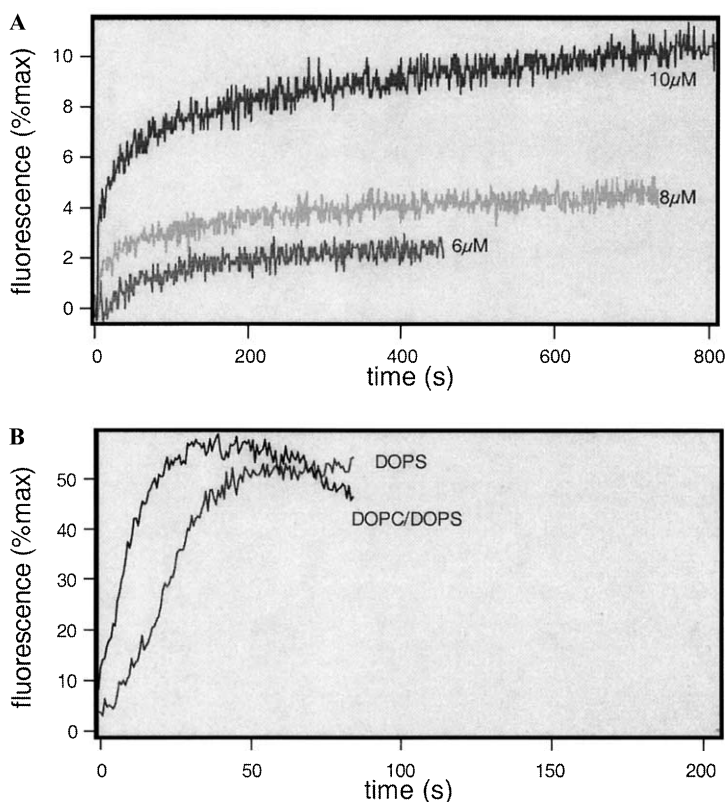


Fig. 1. Fusion monitored by lipid-mixing assays. Fluorescence increase expressed in percentage maximum is measured over time after the addition of the talin peptide in a concentration-dependent manner (A). The peptide is added to a suspension of DOPC/DOPS target and DOPC/cholesterol symmetric donor liposomes containing 1 mol% each of N-NBD-PE and N-Rh-PE as fluorescent lipids. (B) Lipid mixing was induced by the talin peptide coupled with DOPC/cholesterol donor liposomes via PE-PDP. Target liposomes consisted of DOPS or DOPC/DOPS. Dequenching measured as fluorescence increase occurred within seconds.

DOPS vesicles as target population. To discriminate between outer and inner leaflet fusion events we used asymmetrically labeled liposomes. For this purpose, we treated donor liposomes containing both N-Rh-PE and N-NBD-PE with sodium dithionite. Sodium dithionite irreversibly destroys the NBD-fluorescence, thereby eliminating the fluorescent signal derived from N-NBD-PE in the outer leaflet. As a result, the NBD-fluorescence is significantly reduced (compare Fig. 1B with Fig. 2A/DOPS and Fig. 2B/DOPC/DOPS). Changes in fluorescent signals are therefore assumed not to result from lipid exchange in the outer leaflet. Since the kinetic of peptide-induced fluorescence increase of symmetrically and asymmetrically labeled liposomes is similar, it is likely that fusion occurs between outer and inner membrane compartments (compare Fig. 1B with Figs. 2A and B; *Note*. Different timescales).

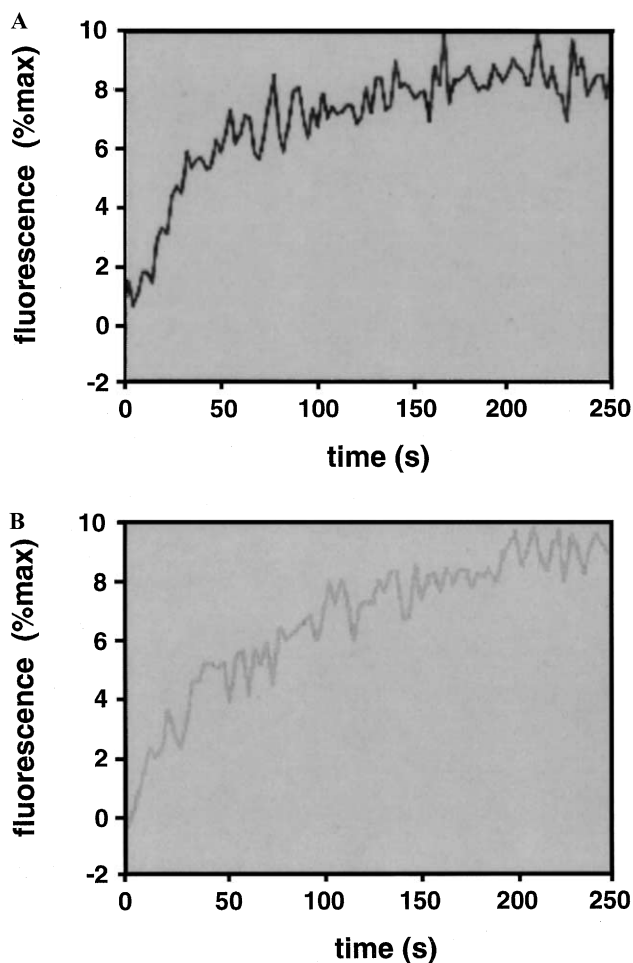


Fig. 2. Fusion monitored of asymmetrically labeled vesicles. (A) Vesicles containing DOPS and (B) DOPC/DOPS. NBD-fluorescence in the outer leaflet is eliminated by dithionite treatment. The fluorescence is reduced by approximately 80% (compare with Fig. 1B). The kinetics of lipid mixing—indicating inner membrane fusion—are similar to that observed for symmetrically labeled vesicles (see Fig. 1B).

### Contents leakage

A pronounced membrane-destabilizing potential of the talin peptide is reflected by leakage assays (Fig. 3). For this purpose we used target vesicles containing 100 mM carboxyfluorescein (CF). Once the peptide is added either free in solution (Fig. 3A) or coupled with donor liposomes (Fig. 3B), dequenching occurs within seconds. The extremely rapid process of leakage gives rise to a maximum fluorescence, and a further increase of fluorescence cannot be achieved after the addition of detergent (arrows in Figs. 3A and B). Since the rate of leakage is significantly faster than that for fusion, as indicated by the lipid-mixing events (compare Figs. 1 and 3), we were unable to measure any contents mixing.

### Cryo-electron microscopy

Cryo-electron microscopy (cryo-EM) provided a first direct indication of talin peptide-induced outer and inner membrane fusion (Fig. 4). Control samples (A) showed dispersed donor (DOPC/cholesterol) and target (DOPC/DOPS) vesicles without the addition of the talin peptide. The average vesicle diameter was 100–150 nm. The addition of 20  $\mu$ M talin led to spontaneous aggregation of vesicles (clustering), as shown in the overview (B). We observed several larger vesicles with a diameter of approximately 200 nm, which most likely resulted from vesicles that had already fused with each other. Figs. 4C–E show individual stages of peptide-induced vesicle fusion events at higher magnification where outer and inner leaflet fusion is clearly recognizable. *Note*. Fig. 4C shows two closely opposed vesicle membranes, a state that most likely precedes actual membrane fusion.

### Molecular modeling of the fusogenic talin peptide at the membrane interface

In comparison with two other predicted talin sequences that may interact with lipid membranes [19,20], the sequence 385–406, with its calculated hydrophobicity of 0.029, high amphipathicity, and hydrophobic moment of 0.3, can be classified as a ‘class B peptide’ according to Brasseur et al. [34]. Using CD-spectroscopy, we experimentally verified that this peptide refolds with a maximal final degree of  $\sim$ 86% from random coil and  $\beta$ -sheet structure into an  $\alpha$ -helix in the presence of lipid vesicles [20]. CD-spectroscopy, a method to investigate the conformational structure of  $\alpha$ -helical peptides, uses the mode of insertion and orientation at the lipid interface by minimizing the interaction energy (sum of van der Waals interactions, torsional potential energy, electrostatic interactions, and lipid transfer energy) [34,35]. Actually, the program shows a segment (amino acid 387–406) without the two N-terminal amino acids (G, E) to be even more suitable for membrane interac-

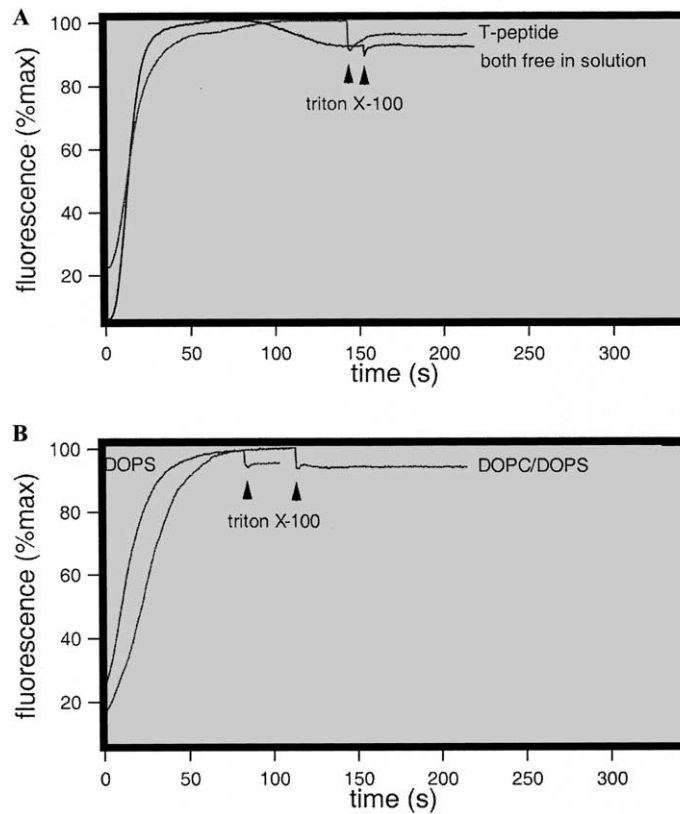


Fig. 3. Fusion induced contents leakage. (A) DOPC/cholesterol liposomes are mixed with DOPS target liposomes containing 100 mM carboxyfluorescein (CF) in the presence of 8  $\mu$ M talin peptide. Rapid leakage is monitored by an immediate increase in fluorescence. Maximal contents leakage is reached as indicated by Triton X-100 treatment (arrows). (B) The peptide is coupled with the donor liposomes via PE-PDP, and the target liposomes consisted of DOPS or DOPC/DOPS, respectively. Conditions as in (A).

tion, since its overall hydrophobicity is calculated to be  $H_0 = 0.13$  and  $\mu H \approx 0.38$  (Table 1). In addition, the highly asymmetrical hydrophobic potential profile along the axis of the  $\alpha$ -helix favors an oblique orientation within the phospholipid bilayer. This is indicated by the molecular graphic in Fig. 5. For peptide 387–406 the angle of insertion was calculated to be  $18^\circ$ . This is consistent with the penetration area of the peptide, which was calculated by the monolayer expansion technique of  $\overset{\circ}{\text{A}}^2 = 160 \pm 15$  for POPC/POPG (3/1) lipid vesicles, a value that exceeds the cross-sectional area of a protein  $\alpha$ -helix [20]. Hence we suggest that, in analogy to viral envelope proteins [35], the major membrane-anchoring peptide (385–406) of talin may insert obliquely at the lipid interface, thereby inducing membrane destabilization, formation of inverse micelles, and membrane fusion events.

## Discussion

Amino acid 385–406 within the N-terminal talin head fragment represents a potential intrinsic membrane-anchoring domain [20]. In the presence of lipids, this membrane anchor exists as an amphipathic  $\alpha$ -helix with

a polybasic motif at one end, enabling membrane partitioning by generating an electrostatic pull on the membrane surface concomitant with the insertion into the hydrophobic phase. Membrane surface charge and lipid-packing pressure obviously are major factors in driving the equilibrium toward the membrane-bound state. At pH 7.4 the total free energy of binding including electrostatic and hydrophobic interactions amounts to  $\Delta G_0 = -9.4$  kcal/mol [20], a value that compares well with that of myristylated membrane-anchoring peptides [36]. The marked hydrophobicity gradient along the axis of the  $\alpha$ -helix, exposing five isoleucines and various other hydrophobic amino acids on one half of the helix, suggests an oblique insertion into the membrane plane (cf. model in Fig. 5). In conjunction with the calculated overall hydrophobicity of  $H_0 = 0.029$  and mean hydrophobic moment of  $\mu H = 0.3$ , the tilted peptide resembles a peptide that was first identified in the envelope protein of several viruses [35]. These peptides are assumed to insert obliquely into a lipid–water interface and are thought to induce a local disorganization of phospholipids by generating new lipid phases and finally membrane fusion. By applying a lipid-mixing assay that relies on resonance energy transfer (RET)-assays, we demonstrated that the major



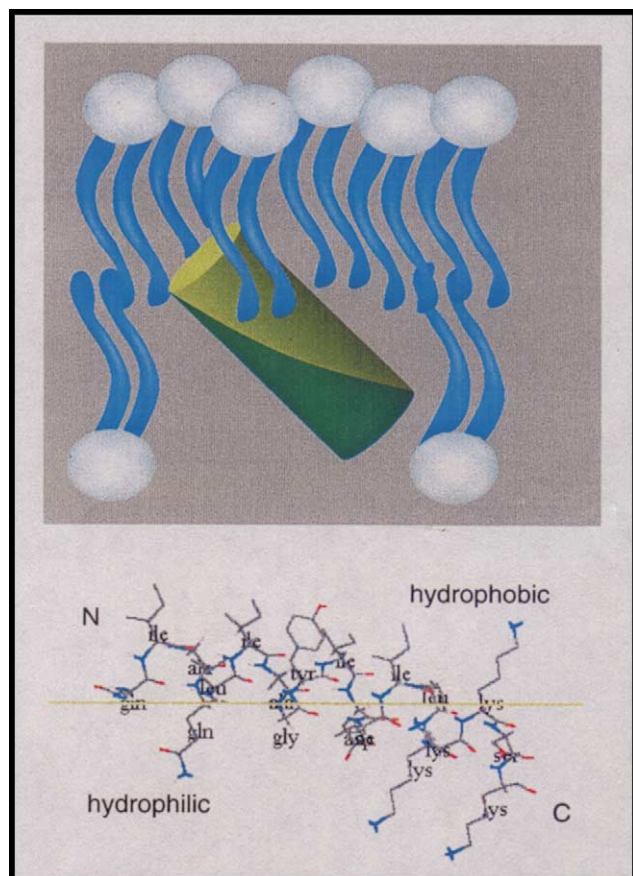


Fig. 5. Molecular modeling of talin peptide interacting with the lipid interface. The strong amphipathic nature of the talin peptide and marked hydrophobicity gradient along its sequence suggests a tilted orientation and a partial penetration of the lipid bilayer favoring destabilization of the phospholipid acyl chains (top). Computer modeling of the mode of insertion of the talin peptide (amino acid 387–406) at the lipid interface as shown in a ribbon diagram. The angle of insertion was calculated to be  $18^\circ$  (bottom).

suggesting that membrane-anchoring domains that have the tendency to induce inverse micelle formation may be responsible for these transitions. Future work will therefore focus on using the intact talin molecule to support our observations. The fact that the calculated binding constants ( $K_d$ ) for the entire molecule [29] and peptide (residues 385–406) [20] with charged lipid vesicles were both in the submolar range is intriguing.

#### Biological implications

**Cell protrusion.** Membrane destabilization via lipid bilayer interaction of an actin-binding protein may be of particular importance for the advancement of the leading edge of moving cells. Displacement of the plasma membrane has to occur during cytoskeletal assembly, which is driven by actin polymerization [38] to allow for the addition of new actin monomers at the membrane-faced barbed end of actin filaments [39,40]. Recently, evidence has emerged that the load against the process

works depends on membrane tension [41]. It is possible that the rate of extension is inversely proportional to plasma membrane tension in living cells. In addition, it was shown that the resisting force of the membrane surface may be lowered by adding detergent or large amounts of phospholipids. The rate of lamellipodial extension is also increased by amphiphilic compounds that partition into the plasma membrane. This shows that in addition to biochemical receptor pathways, physical parameters may also play a role in cell signaling [42]. A decrease in the resistance of the plasma membrane could lead to an enhancement of Brownian motion and thus allow fluctuation of the membrane itself as well as deflection of assembling filaments [41,42]. This process is best described by the Brownian-ratchet model [43]. Since talin is concentrated at the tips of nascent actin filament bundles in moving cells [5] and has been shown to nucleate actin polymerization *in vitro* [9], its involvement in cytoskeleton assembly appears most likely.

**Cytotic events.** Assuming particle movement on the cell surface, it is suggested that membrane flow is coupled with cell protrusion [44]. There is evidence that a balance of exocytosis driven from an intracellular reservoir at the leading edge and endocytosis occurring more rearward may underlie membrane dynamics [45,46]. Fusogenic properties of a cytoskeleton-linked membrane-associated protein could thus be important for targeting intracellular vesicles toward assembly sites in leading lamellae. Further *in vivo* studies are needed to establish such a link.

#### Acknowledgments

The authors like to thank Dr. Belinda Vanloo for computer modeling, and Drs. Eve-Isabelle Pécheur and Jochen Boehm for their technical assistance, and Judith Feldmann, Ph.D. for critical reading of the manuscript. This work was supported by the Deutsche Forschungsgemeinschaft (DFG, Grant IS 25/8-1) and by a Collaborative Research Grant from NATO. Excerpts from this paper have been presented at the ASCB meeting in Washington 2001.

#### References

- [1] D.J. Rees, S.E. Ades, S.J. Singer, R.O. Hynes, Sequence and domain structure of talin, *Nature (London)* 347 (1990) 685–689.
- [2] A. Bretscher, D. Deczek, M. Berryman, Ezrin: a protein requiring conformational activation to link microfilaments to the plasma membrane in the assembly of cell surface structures, *J. Cell Sci.* 110 (1997) 3011–3018.
- [3] M.J. Belliveau, M. Lutchman, J.O. Claudio, C. Mariveau, G.A. Rouleau, Schwannomin: new insights into this member of the band 4.1 superfamily, *Biochem. Cell Biol.* 73 (1995) 733–737.
- [4] K. Burridge, L. Connell, A new protein of adhesion plaques and ruffling membranes, *J. Cell Biol.* 97 (1983) 359–367.
- [5] J.A. De Pasquale, C.S. Izzard, Accumulation of talin in nodes at the edge of the lamellipodium and separate incorporation into

- adhesion plaques at focal contacts in fibroblasts, *J. Cell Biol.* 113 (1991) 1351–1359.
- [6] M.C. Beckerle, D.E. Miller, M.E. Bertagnoli, S.J. Locke, Activation-dependent redistribution of the adhesion plaque protein, talin, in intact human platelets, *J. Cell Biol.* 109 (1989) 3333–3346.
- [7] M. Muguruma, S. Matsumura, T. Fukazawa, Direct interactions between talin and actin, *Biochem. Biophys. Res. Commun.* 171 (1990) 1217–1223.
- [8] W.H. Goldmann, G. Isenberg, Kinetic determination of talin-actin binding, *Biochem. Biophys. Res. Commun.* 178 (1991) 718–723.
- [9] S. Kaufmann, T. Piekenbrock, W.H. Goldmann, M. Baermann, G. Isenberg, Talin binds to actin and promotes filament nucleation, *FEBS Lett.* 284 (1991) 187–191.
- [10] V. Niggli, S. Kaufmann, W.H. Goldmann, T. Weber, G. Isenberg, Identification of functional domains in the cytoskeletal protein talin, *Eur. J. Biochem.* 224 (1994) 951–957.
- [11] L. Hemmings, D.J.G. Rees, V. Ohanian, S.J. Bolton, A.P. Gilmore, B. Patel, H. Priddle, J.E. Trevithick, R.O. Hynes, D.R. Critchley, Talin contains three actin-binding sites each of which is adjacent to a vinculin-binding site, *J. Cell Sci.* 109 (1996) 2715–2726.
- [12] R.O. McCann, S.W. Craig, The I/LWEQ module: a conserved sequence that signifies F-actin binding in functionally diverse proteins from yeast to mammals, *Proc. Natl. Acad. Sci. USA* 94 (1997) 5679–5684.
- [13] W.H. Goldmann, D. Hess, G. Isenberg, The effect of intact talin and talin tail fragment on actin filament dynamics and structure depends on pH and ionic strength, *Eur. J. Biochem.* 260 (1999) 439–445.
- [14] A. Horwitz, K. Duggan, C. Buck, M.C. Beckerle, K. Burridge, Interaction of plasma membrane fibronectin receptor with talin—a transmembrane linkage, *Nature (London)* 320 (1986) 531–533.
- [15] I. Knezevic, I. Leisner, S.C.-T. Lam, Direct binding of the platelet integrin  $\alpha\text{IIb}\beta\text{3}$  (GPIIb-IIIa) to talin. Evidence that interaction is mediated through the cytoplasmic domains of both  $\alpha\text{IIb}$  and  $\beta\text{3}$ , *J. Biol. Chem.* 271 (1995) 16416–16421.
- [16] K. Burridge, P. Mangeat, An interaction between vinculin and talin, *Nature (London)* 308 (1984) 744–746.
- [17] M.L. Borowsky, R.O. Hynes, Layilin, a novel talin-binding transmembrane protein homologous with C-type lectins, is localized in membrane ruffles, *J. Cell Biol.* 143 (1998) 429–442.
- [18] D.A. Calderwood, R. Zent, R. Grant, D.J.G. Rees, R.O. Hynes, M.H. Ginsburg, The talin head domain binds to integrin  $\beta$  subunit cytoplasmic tails and regulates integrin activation, *J. Biol. Chem.* 274 (1999) 28071–28074.
- [19] M. Tempel, W.H. Goldmann, G. Isenberg, E. Sackmann, Interaction of the 47-kDa talin fragment and the 32-kDa vinculin fragment with acidic phospholipids: a computer analysis, *Biophys. J.* 69 (1995) 228–241.
- [20] A. Seelig, X. Li Blatter, A. Frentzel, G. Isenberg, Phospholipid binding of synthetic talin peptides provides evidence for an intrinsic membrane anchor of talin, *J. Biol. Chem.* 275 (2000) 17954–17961.
- [21] F.J. Martin, T.D. Heath, R.R.C. New, in: R.R.C. New (Ed.), *Liposomes: A Practical Approach*, IRL Press, Oxford, 1990, pp. 162–182.
- [22] E.-I. Pécheur, D. Hoekstra, J. Saint-Marie, L. Maurin, A. Bienvenue, J.R. Phillipot, Membrane anchorage brings about fusogenic properties in a short synthetic peptide, *Biochemistry* 36 (1997) 3773–3781.
- [23] D.K. Struck, D. Hoekstra, R.E. Pagano, Use of resonance energy transfer to monitor membrane fusion, *Biochemistry* 20 (1981) 4093–4099.
- [24] D. Hoekstra, R. Buist-Arkema, K. Klappe, C.P.M. Reutelink-sperger, Interaction of annexins with membranes: the N-terminus as a governing parameter as revealed with a chimeric annexin, *Biochemistry* 32 (1993) 14194–14202.
- [25] J.C. McIntyre, R.G. Sleight, Fluorescence assay for phospholipid membrane asymmetry, *Biochemistry* 30 (1991) 11819–11827.
- [26] J.N. Weinstein, S. Yoshikami, P. Henkart, R. Blumenthal, W.A. Hagins, Liposome-cell interaction: transfer and intracellular release of a trapped fluorescent marker, *Science* 195 (1977) 489–491.
- [27] J. Dubochet, M. Adrian, J. Chang, J.C. Homo, J. Lepault, A.W. McDowell, P. Schulz, Cryo-electron microscopy of vitrified specimens, *Quart. Rev. Biophys.* 21 (1988) 129–228.
- [28] R. Grimm, H. Singh, R. Rachel, D. Typke, W. Zillig, W. Baumeister, Electron tomography of ice-embedded prokaryotic cells, *Biophys. J.* 74 (1998) 1031–1042.
- [29] D. Eisenberg, R.M. Weiss, T.C. Terwilliger, The hydrophobic moment detects periodicity in protein hydrophobicity, *Proc. Natl. Acad. Sci. USA* 81 (1984) 140–144.
- [30] R. Bresseur, Differentiation of lipid-associating helices by use of three-dimensional molecular hydrophobicity potential calculations, *J. Biol. Chem.* 266 (1991) 16120–16127.
- [31] R. Bresseur, M. Vandenbranden, B. Cornet, J.-M. Ruyschaert, Orientation into the lipid bilayer of an asymmetric amphipathic helical peptide located at the N-terminus of viral fusion proteins, *Biochim. Biophys. Acta* 1029 (1990) 267–273.
- [32] W.H. Goldmann, R. Senger, S. Kaufmann, G. Isenberg, Determination of the affinity of talin and vinculin to charged lipid vesicles: a light scatter study, *FEBS Lett.* 368 (1995) 516–518.
- [33] C. Dietrich, W.H. Goldmann, E. Sackmann, G. Isenberg, Interaction of NBD-talin with lipid monolayers. A film balance study, *FEBS Lett.* 324 (1993) 37–40.
- [34] R. Bresseur, T. Pillot, L. Lins, J. Vandekerckhove, M. Rosseneu, Peptides in membranes: tipping the balance of membrane stability, *Trends Biochem. Sci.* 22 (1997) 167–171.
- [35] R. Bresseur, B. Vanloo, R. Deleys, I. Lins, C. Laheur, J. Taveirne, J.-M. Ruyschaert, M. Rosseneu, Synthetic model peptides for apolipoproteins. I. Design and properties of synthetic model peptides for the amphipathic helices of the plasma apolipoproteins, *Biochim. Biophys. Acta* 1170 (1993) 1–7.
- [36] R.M. Peitzch, S. McLaughlin, Binding of acylated peptides and fatty acids to phospholipid vesicles: pertinence to myristoylated proteins, *Biochemistry* 32 (1993) 10436–10443.
- [37] A. Saitoh, K. Takiguchi, Y. Tanaka, H. Hotani, Opening-up of liposomal membranes by talin, *Proc. Natl. Acad. Sci. USA* 95 (1998) 1026–1031.
- [38] A. Mogilner, G. Oster, Cell motility driven by actin polymerization, *Biophys. J.* 71 (1996) 3030–3045.
- [39] J.V. Small, G. Isenberg, J.E. Celis, Polarity of actin at the leading edge of cultured cells, *Nature (London)* 272 (1978) 638–639.
- [40] V.C. Abraham, V. Krishnamurthi, D.L. Taylor, F. Lanni, The actin-based nanomachine at the leading edge of migrating cells, *Biophys. J.* 77 (1999) 1721–1732.
- [41] D. Raucher, M. Sheetz, Cell spreading and lamellipodial extension rate is regulated by membrane tension, *J. Cell Biol.* 148 (2000) 127–136.
- [42] G. Isenberg, New concepts for signal perception and transduction by the actin skeleton at cell boundaries, *Semin. Cell Dev. Biol.* 7 (1996) 707–715.
- [43] C.S. Peskin, G.M. Odell, G.F. Oster, Cellular motions and thermal fluctuations: the Brownian ratchet, *Biophys. J.* 65 (1993) 316–324.
- [44] M. Abercrombie, J.E. Heaysman, S.M. Pegrum, The locomotion of fibroblasts in culture. 3. Movements of particles on the dorsal surface of the leading lamella, *Exp. Cell Res.* 62 (1970) 389–398.
- [45] M.S. Bretscher, Moving membrane up to the front of migrating cells, *Cell* 87 (1996) 601–606.
- [46] J. Dai, M.P. Sheetz, Axon membrane flows from the growth cone to the cell body, *Cell* 83 (1995) 693–701.